Journal of Engineering Mathematics **39:** 63–78, 2001.

Microwave joining of two long hollow tubes: an asymptotic theory and numerical simulations

GREGORY A. KRIEGSMANN and JONATHAN H.C. LUKE
Department of Mathematical Sciences, Center for Applied Mathematics and Statistics, New Jersey Institute of Technology, University Heights, Newark, NJ 07102, U.S.A.

Received 25 November 1999; accepted in revised form 2 May 2000

Abstract. A nonlinear heat equation which models the microwave assisted joining of two large SiC tubes is analyzed. By exploiting the small fineness ratio of the structure and disparate time scales an asymptotic theory for this problem is systematically deduced. Specifically, a one-dimensional nonlinear heat equation is described which governs the temperature in the outer region. This is a numerically well posed problem and it is efficiently solved using standard methods. This solution is not valid in the inner region which includes the microwave source. An inner asymptotic approximation is derived to describe the temperature in this region. This approximation yields two unknown functions which are determined from matching to the outer solution. The results of the asymptotic theory are compared to calculations done on the full problem. Since the full problem is numerically ill conditioned, the asymptotic theory yields enormous savings in computational time and effort.

Key words: microwaves, matched asymptotic methods, ceramics, joining, heat transfer

1. Introduction

The use of microwaves to join ceramics has received a considerable amount of study over the past several years [1–3]. Problems of practical and theoretical interest occur on both the microscopic and macroscopic levels. The microstructure and integrity of the bonding region and the mechanical strength of ceramic joints are important questions that must be resolved on the microscopic level. However, problems on the macroscopic level that include localizing the electric field in the joint region and determining, *a priori*, the temperature distribution at the joint and the surrounding material have a profound influence on the micro-processes that occur during joining. It is this macroscopic description that we address here for the specific application of joining two hollow cylinders of silicon carbide, such as might be used as radiant burner tubes for heat treating of metals.

The mathematical model that we build here focuses only on the heat transfer aspects of the joining process. Specifically we assume that the electric field present in the microwave cavity is completely specified by the lowest mode and is independent of the material being heated. This assumption is a good first order approximation for thin walled tubes in a nominally resonant cavity. The mathematical statement of the problem is then a nonlinear initial value problem for the heat equation with a source that incorporates the modal structure of the electric field. The nonlinearity arises from radiative heat transport on the surface of the hollow cylinders which is important at joining temperatures.

Although the initial boundary value problem is fairly straightforward to solve numerically, even with the nonlinear losses, there are several features of this problem which mitigate against a frontal numerical attack. First, the aspect ratio of the hollow tube is very small. For the radiant tube mentioned above the outer radius is 2in. and its length is 4ft giving an aspect ratio of $\frac{1}{24}$. Thus, the initial boundary value problem must be solved in a long skinny domain which manifests itself as a small parameter that multiplies the axial diffusion term. This makes the problem nearly singular and numerically ill-posed. Secondly, there are three time scales in the problem, two of the same order and the other much smaller. Specifically for the present application the radial diffusion time is much smaller than the axial diffusion time which is of the same order as the convective time. This later time is a measure of how quickly the tube will cool in the absence of the electric source. The disparity of the time scales causes another computational problem. To capture the thermal dynamics on the shortest time scale, *i.e.*, radial diffusion, numerical integration must continue for a very long time until the physical effects on the long time scale become dominant.

We present here an analysis of this problem which is based on the method of matched asymptotic expansions [4] which exploits the small fineness ratio and disparate time scales. In the inner region, within and near the cavity, we derive an expansion which captures the physics of the heating process. This expansion becomes invalid outside the cavity and it contains undetermined functions which depend upon time. We then construct an outer expansion valid away from the cavity. The leading order term satisfies a one-dimensional axial heat equation with a loss term that models radiative and convective heat transfer. The first order correction satisfies a linear version of this equation. In both cases boundary conditions are prescribed at one end of the cylinder, but not at the other which corresponds to the cavity. Matching is then applied to determine these boundary conditions. The first order correction is proved to be identically zero and the leading order equation must be solved numerically. Once this is done, the unknown functions of time in the inner region are uniquely determined.

The asymptotic scheme we present here is closely related to others that have appeared in the literature. Specifically our exploitation of the disparity between the radial diffusion and convective time scales (*i.e.*, a small Biot number) has been done in the context of FZ silicon processing [5]. In fact the matching performed in this paper is similar to ours with the solid-liquid inner region corresponding to our cavity region. Perhaps our method is more closely related to the schemes developed to study thermal-solutal diffusion in float zones [6] and Ohno continuous casting of cored rods [7]. These asymptotic schemes, and ours, exploit both the smallness of the fineness ratio and Biot number. However, our problem is time dependent and these previous works were not. This additional feature is important in ceramic joining where the time history of the temperature plays an important role in determining the microstructure of the joint [3].

Returning to the results of our paper, the one-dimensional nonlinear heat equation that describes the leading order term in the outer expansion is numerically well posed. Thus, an accurate approximation can easily be constructed in this region. This, coupled with the analytic information contained in the inner expansion, yields an efficient and accurate description of the heating process. We also perform a direct numerical attack on this problem for comparison. Because of the singular nature of the equations this direct numerical approach takes much longer to solve than the one-dimensional heat equation, about three orders of magnitude. The results of the direct numerical calculations and those of our asymptotic method agree almost exactly with errors that are in concert with our asymptotic remainders.

In summary the problem we present here is a simplified model of a real physical experiment. Although certain effects are neglected we believe that it does capture many of the important physical features of the real problem. Moreover, it provides an excellent example

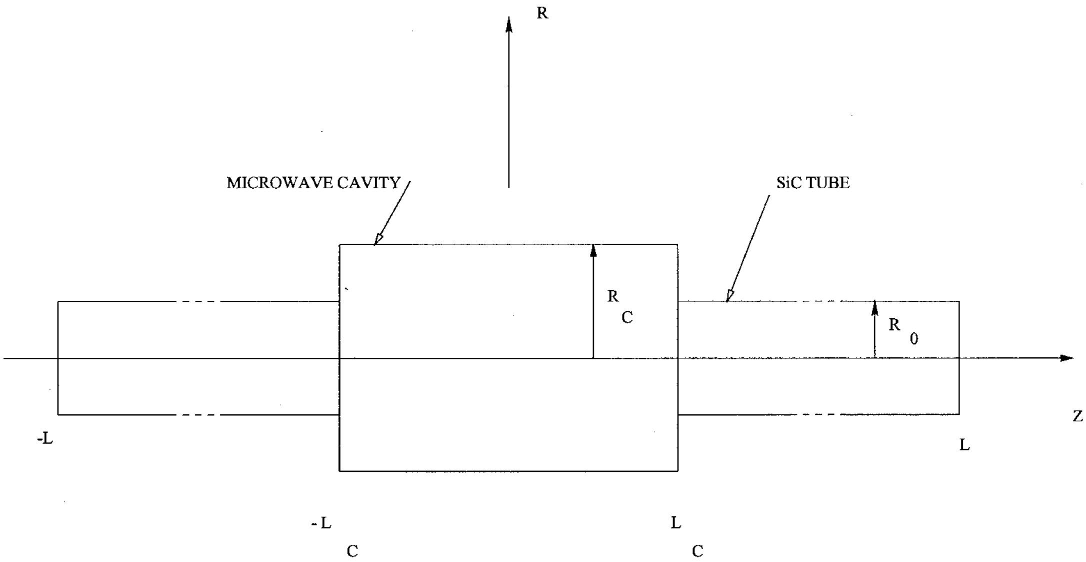

Figure 1. Geometrical sketch.

of how asymptotic analysis can reduce a complicated problem to a simpler one which is amenable to numerical simulation.

2. Problem formulation

Two hollow identical SiC tubes of length L are brought together in perfect thermal contact at $Z = 0$. The inner radius of each tube is R_i, the outer, R_0. A cylindrial cavity of radius $R_C > R_0$, centered at $Z = 0$, encloses the portion of the joined pipes between $\pm L_C$. Microwaves are introduced into the cavity by external circuitry and are contained therein. The setup is shown schematically in Figure 1.

The temperature in the pipes is governed by the heat equation

$$\rho C_P \frac{\partial}{\partial T} = K\nabla^2 T + \frac{\sigma}{2}|\mathbf{E}|^2, \quad |Z| < L, \quad R_i < R < R_0, \tag{1a}$$

$$K\frac{\partial}{\partial R}T = -S(T), \quad R = R_0; \quad S(T) \approx h(T - T_A) + s\epsilon_0(T^4 - T_A^4), \tag{1b}$$

$$K\frac{\partial}{\partial R}T = 0, \quad R = R_i, \tag{1c}$$

$$T = T_A, \quad Z = \pm L, \tag{1d}$$

$$T(X, Y, Z, 0) = T_A, \tag{1e}$$

where ρ is the density, C_P the thermal capacity, K the thermal conductivity, and σ the effective electrical conductivity of the tube, respectively. The parameter h is the effective heat transfer coefficient, s is the Boltzmann constant, ϵ_0 is the emissivity of the tube, T_A is the temperature of the ambient air in which the joined pipes are situated, and $|\mathbf{E}|$ is the amplitude of the electric field.

There are several points that must be made at this junction. First, the thermal parameters and the effective electrical conductivity are taken to be independent of temperature. This is a reasonable assumption for highly conductive materials, such as SiC. However, for other materials this temperature dependence is important and this point will be revisited in Section 6. Secondly, the thermal boundary condition at $R = R_0$ takes into account both convective and radiative heat loss, the later being dominant at the joining temperature T_J. Finally, the thermal boundary condition at $R = R_i$ assumes that neither radiative nor convective losses are important at this surface. This assumption will also be revisited in Section 6 this paper.

To finish the mathematical description of the problem, we must make assumptions regarding the electric field in the cavity. The determination of the field from first principles requires the solution of Maxwell's equations in a complicated cavity composed of the metallic walls, the SiC cylinders, and feeding antennae which couple the microwave power into the cavity. This problem is quite involved and requires a numerical resolution. Once the electric field is known throughout the cavity, then (1) is solved for the temperature distribution. It is the later problem that we focus on in this paper; accordingly we shall simply specify the source term $|\mathbf{E}|^2$ as

$$|\mathbf{E}|^2 = E_0^2 S(\pi Z/2L_C) P(\omega_1 R/R_C), \tag{2a}$$

$$S(\pi Z/2L_C) = \cos^2(\pi Z/2L_C) H(-|Z| + L_C), \quad R_i < R < R_0, \tag{2b}$$

$$P(\omega_1 R/R_C) = J_1^2(\omega_1 R/R_C), \quad |Z| < L_C, \tag{2c}$$

where E_0^2 is a measure of the microwave power, J_1 is the Bessel function of order 1 and ω_1 its first zero, and H is the Heaviside function. The cosine and Bessel function in (2) model the lowest mode in the cavity (TE_{101}) and the Heaviside function crudely models the other aspect of the cavity which confines the electric field to its interior. This neglects the chokes that are appended to the cavity (through which the pipes must pass) and their effect of exponentially attenuating the electric field. Again, this simple choice of $|\mathbf{E}|^2$ allows us to focus on the thermal aspects of the joining problem.

Before closing this section we will rewrite (1–2) in a dimensionless form. This is a necessary first step in both our asymptotic and numerical analyses that will follow. We begin by introducing the dimensionless variables

$$r = R/R_0, \quad z = Z/L, \quad \eta = t/\theta, \quad u = (T - T_A)/T_A \tag{3a}$$

and by defining the dimensionless parameters

$$\begin{aligned} &\theta_C = \rho C_P R_0/h, \quad \theta = \rho C_P L^2/K, \quad \alpha = \theta/\theta_C, \quad \theta_R = \rho C_P R_0^2/K, \\ &\epsilon = R_0/L, \quad \gamma = \omega_1 R_0/R_C, \quad \chi = \frac{\pi}{2}\frac{R_0}{L_C}, \quad r_1 = \frac{R_i}{R_0}, \\ &\beta = s\epsilon_0 T_A^3/h, \quad q = [\sigma E_0^2/2][R_0 L/K T_A], \quad L(u) = u + \beta[(u+1)^4 - 1]. \end{aligned} \tag{3b}$$

Here θ_C is a time scale associated with convective losses, θ is a time scale associated with axial diffusion and θ_R with radial diffusion. $L(u)$ is the dimensionless power lost by radiation and convection, β is the ratio of radiative to convective power lost at the surface, and ϵ is the fineness ratio of the cylinder. For a typical SiC joining experiment we take $L = 4$ft, $R_0 = 2$in, $R_i = 1{\cdot}75$in, $L_C = 6$in, $R_C = 3{\cdot}9$in, $h = 10\mathrm{W/m^{2\circ}K}$, $K = 100\mathrm{W/m^\circ K}$, $\epsilon_0 = {\cdot}75$, and $s = 5{\cdot}67 \times 10^{-9}\mathrm{W/m^{2\circ}K}$. This implies that all the parameters defined above are $O(1)$ except $\epsilon \sim 0{\cdot}04$. In particular the scaling $\alpha = O(1)$ states the physical fact that $\theta_R/\theta_C = 0(\epsilon^2)$, *i.e.*, the radical and axial diffusive time scales are disparate. Finally, we have chosen $R_C = 3{\cdot}9$in so that the maximum of J_1^2 occurs at $R = 1{\cdot}875$in, *i.e.*, at the midpoint of the tube wall.

Using the definitions defined in (3) we find that (1–2) take the dimensionless form

$$\epsilon^2 \frac{\partial}{\partial \eta} u = \frac{\partial^2}{\partial r^2} u + \frac{1}{r}\frac{\partial}{\partial r} u + \epsilon^2 \frac{\partial^2}{\partial z^2} u + q\epsilon S(\chi \frac{z}{\epsilon}) P(\gamma r), \tag{4a}$$

$$\frac{\partial}{\partial r} u + \alpha\epsilon^2 L(u) = 0, \quad r = 1, \quad \frac{\partial}{\partial r} u = 0, \quad r = r_1 \tag{4b}$$

$$u = 0, \quad z = 1, \tag{4c}$$

$$u = 0, \quad \eta = 0. \tag{4d}$$

The appearance of the small parameter ϵ^2 in front of the time derivative and the second order spatial derivative implies that the solution is singular in the limit as $\epsilon \to 0$. This is further suggested by the singular character of S in this limit. It is precisely this characteristic which makes the initial, boundary-value problem (4) ill conditioned for direct numerical simulations.

3. Asymptotic analysis

In this section we will construct an asymptotic approximation of the solution to (4) in the limit as $\epsilon \to 0$ with all the other parameters in the problem fixed and $O(1)$. This will be done in several stages. First, we shall construct an ‘inner’ approximation which is valid near the cavity where $z \sim O(\epsilon)$ or equivalently where $Z \sim L_C$. In the second stage we will derive an ‘outer approximation’ which is valid away from the cavity. Finally, we will use matching to determine the various unknown terms in the inner and outer expansions and thus obtain a complete description of the temperature distribution in the cylinders.

We note here that time has been scaled so that (4) describes the evolution of the temperature on the longest time scale where convection and axial diffusion are the dominant heat transfer mechanisms. This occurs when $\eta \sim 0(1)$ or equivalent, $t \sim \theta$. Since the temperature will evolve to a steady state on this time scale, it is the most important for a joining application. However, there is a possibility that features on the shortest time scale, where radial diffusion dominates, will not be captured by (4). This would occur when $t \sim \theta_R$ or equivalently, when $\eta \sim 0(\epsilon^2)$. The inability of (4) to describe the temperature evolution on this short time scale will mathematically manifest itself as an initial time layer of thickness $O(\epsilon^2)$ where the asymptotic approximation deduced from (4) will become invalid. This nonuniformity will be addressed and a remedy will be described in Section 3.4.

3.1. The inner expansion

We begin by defining the inner axial variable $\bar{z} = z/\epsilon$ which we take as $O(1)$. This is equivalent to $Z \sim L_C$. Inserting this change of variables into (4) gives

$$\epsilon^2 \frac{\partial}{\partial \eta} u = \frac{\partial^2}{\partial r^2} u + \frac{1}{r}\frac{\partial}{\partial r} u + \frac{\partial^2}{\partial \bar{z}^2} u + q\epsilon S(\chi \bar{z}) P(\gamma r), \quad r_1 < r < 1, \quad 0 < \bar{z} < \infty, \tag{5a}$$

$$\frac{\partial}{\partial r} u + \alpha\epsilon^2 L(u) = 0, \quad r = 1, \quad \frac{\partial}{\partial r} u = 0, \quad r = r_1, \tag{5b}$$

$$\frac{\partial}{\partial \bar{z}} u = 0, \quad \bar{z} = 0, \tag{5c}$$

$$u = 0, \quad \eta = 0. \tag{5d}$$

We observe that the source function S, the Equation (5a), boundary conditions (5b), and initial condition (5d) are symmetric in $\bar{z}$ so that we need only solve the problem on the half interval $\bar{z} > 0$. This symmetric is reflected in the Neumann boundary condition (5c). We next expand u in the asymptotic series

$$u = \sum_{n=0}^{\infty} u_n(r, \bar{z}, \eta)\epsilon^n. \tag{6}$$

Inserting this expansion into (5), expanding the nonlinear term using a Taylor series expansion, and equating to zero the coefficients of the powers of ϵ yields an infinite set of equations. These sequentially determine $u_n(r, \bar{z}, \eta)$. We shall just list the first three which are sufficient to deduce u to $O(\epsilon^2)$. They are:

$$\bar{\nabla}^2 u_0 = 0, \quad r_1 < r < 1, \quad 0 < \bar{z} < \infty, \tag{7a}$$

$$\frac{\partial}{\partial r} u_0 = 0, \quad r = r_1, 1, \tag{7b}$$

$$\frac{\partial}{\partial \bar{z}} u_0 = 0, \quad \bar{z} = 0; \quad u_0 = 0, \eta = 0, \tag{7c}$$

$$\bar{\nabla}^2 u_1 = -qS(\chi \bar{z}) P(\gamma r), \quad r_1 < r < 1, \quad 0 < \bar{z} < \infty, \tag{8a}$$

$$\frac{\partial}{\partial r} u_1 = 0, \quad r = r_1, 1, \tag{8b}$$

$$\frac{\partial}{\partial \bar{z}} u_1 = 0, \quad \bar{z} = 0; \quad u_1 = 0, \eta = 0, \tag{8c}$$

$$\bar{\nabla}^2 u_2 = \frac{\partial}{\partial \eta} u_0, \quad r_1 < r < 1, \quad 0 < \bar{z} < \infty, \tag{9a}$$

$$\frac{\partial}{\partial r} u_2 = 0, \quad r = r_1, \frac{\partial}{\partial r} u_2 = -\alpha L(u_0), \tag{9b}$$

$$\frac{\partial}{\partial \bar{z}} u_2 = 0, \quad \bar{z} = 0; \quad u_2 = 0, \eta = 0, \tag{9c}$$

where $\bar{\nabla}^2$ is the Laplacian operator in r and $\bar{z}$.

The solution to the boundary value problem (7) is just $u_0 = a_0(\eta)$. This function is unknown at this stage of our analysis. The boundary value problem (8) is more involved. Its solution is given by the expansion

$$u_1 = b_0 \psi_0 + \sum_{m=1}^{\infty} b_m(\bar{z}, \eta) \psi_m(r), \tag{10a}$$

where the eigenfunctions ψ_m satisfy

$$\frac{d^2 \psi_m}{dr^2} + \frac{1}{r} \frac{d\psi_m}{dr} + \lambda_m \psi_m = 0, \tag{10b}$$

$$\frac{d\psi_m}{dr} = 0, \quad r = r_1, 1. \tag{10c}$$

This is a regular Sturm Liouville problem; accordingly the eigenfunctions ψ_m form an orthonormal set and their corresponding eigenvalues are real and ordered, $\lambda_0 < \lambda_1$..... In fact the lowest eigenvalue $\lambda_0 = 0$ and the corresponding eigenfunction $\psi_0 = \sqrt{\frac{2}{1-r_1^2}}$, *i.e.*, a constant. We find from (10) and (8) that the functions b_m satisfy the ordinary differential equations

$$\frac{d^2 b_m}{d\bar{z}^2} - \lambda_m b_m = -q S(\chi \bar{z}) P_m, \tag{11a}$$

$$\frac{db_m}{d\bar{z}} = 0, \quad \bar{z} = 0, \tag{11b}$$

$$P_m = \int_{r_1}^{1} \psi_m P(\gamma r) r dr \equiv \langle \psi_m, P \rangle \tag{11c}$$

The solutions to these simple boundary value problems are

$$b_0 = a_1(\eta) - q P_0 \int_0^{\bar{z}} (\bar{z} - p) S(\chi p) dp, \tag{12a}$$

$$b_m = \gamma_m \cosh \beta_m \bar{z} - \frac{q P_m}{\beta_m} \int_0^{\bar{z}} \sinh \beta_m (\bar{z} - p) S(\chi p) dp, \tag{12b}$$

where $\beta_m = \sqrt{\lambda_m}$, $\quad \bar{z}_c = Z_C / R_0$, and

$$\gamma_m = \frac{q P_m}{\beta_m} \int_0^{\bar{z}_C} S(\chi p) e^{-\beta_m p} dp. \tag{12c}$$

The constant γ_m is chosen so that b_m decays exponentially as $\bar{z} \to \infty$, a condition that is later required for matching, and the function $a_1(\eta)$ is unknown at this stage of the analysis.

The solution to the boundary value problem (9) is determined along similar lines. Omitting the details of the analysis we simply state the result

$$u_2 = ar + \frac{b}{2}r^2 + [a_2(\eta) + c_0]\psi_0 + \sum_{m=1}^{\infty} c_m(\bar{z}, \eta)\psi_m(r), \tag{13a}$$

$$a = \frac{\alpha r_1}{1 - r_1} L(u_0), \quad b = \frac{-\alpha}{1 - r_1} L(u_0), \tag{13b}$$

$$c_0\psi_0 = \frac{\bar{z}^2}{2}\Delta_0; \quad \Delta_0 = \frac{\mathrm{d}u_0}{\mathrm{d}\eta} - 2b - a\psi_0^2(1 - r_1), \tag{13c}$$

$$c_m = \frac{\Delta_m}{\lambda_m}; \quad \Delta_m = -a\int_{r_1}^{1} \psi_m \mathrm{d}r, \quad m \geq 1, \tag{13d}$$

where $a_2(\eta)$ is unknown at this stage of the analysis.

Combining (10a) and 13a) with (6) gives the inner expansion

$$\begin{aligned} u = \; & a_0(\eta) + \epsilon\left[\sum_{m=0}^{\infty} b_m\psi_m\right] \\ & + \epsilon^2\left[ar + \frac{b}{2}r^2 + a_2(\eta)\psi_0 + c_0\psi_0 + \sum_{m=1}^{\infty} c_m(\bar{z}, \eta)\psi_m(r)\right] + O(\epsilon^3), \end{aligned} \tag{14}$$

where $O(\epsilon^3)$ represents the contributions of the higher order terms. We shall need the far field expansion, *i.e.*, $\bar{z} >> 1$, of this expansion shortly. It is easily deduced to be

$$\begin{aligned} u = \; & a_0(\eta) + \epsilon[a_1(\eta) + qP_0(d_1 - d_0\bar{z})]\psi_0 \\ & + \epsilon^2\left[ar + \frac{b}{2}r^2 + a_2(\eta)\psi_0 + \frac{\bar{z}^2}{2}\Delta_0 + \sum_{m=1}^{\infty} \frac{\Delta_m}{\lambda_m}\psi_m\right], \end{aligned} \tag{15a}$$

$$\mathrm{d}_0 = \int_0^{\bar{z}_c} S(\chi P)\mathrm{d}p, \quad \mathrm{d}_1 = \int_0^{\bar{z}_c} pS(\chi P)\mathrm{d}p, \tag{15b}$$

where exponentially small terms have been neglected. The constant parameter $qP_0\mathrm{d}_0$ is related to the total power supplied by the microwave source and $qP_0\mathrm{d}_1$ to its first moment. It is clear from the linear and quadratic terms in this expression that (14) is not a uniform asymptotic expansion. Another representation must be found and this is the subject of the next section.

3.2. The outer expansion

We now seek an asymptotic expansion of the original problem (4) when $z = 0(1)$. The source term in (4a) is zero when z is restricted in this faction. We again expand u in an asymptotic expansion

$$u = \sum_{m=0}^{\infty} w_m(r, z, \eta)\epsilon^m, \tag{16}$$

where the coefficients w_m now depend on the outer variable z. Inserting this expansion into (4), expanding the nonlinear term using a Taylor series expansion, and equating to zero the coefficients of the powers of ϵ yields an infinite set of equations. These sequentially determine $w_m(r, z, \eta)$. We shall just list the first four which are sufficient to deduce u to $O(\epsilon^2)$. They are:

$$\frac{\partial^2}{\partial r^2}w_j + \frac{1}{r}\frac{\partial}{\partial r}w_j = 0, \quad r_1 < r < 1, \quad 0 < z < 1, \tag{17a}$$

$$\frac{\partial}{\partial r}w_j = 0, \quad r = r_1, 1, \tag{17b}$$

$$w_j = 0, \quad z = 1; \quad w_j = 0, \quad \eta = 0 \tag{17c}$$

for $j = 0, 1$,

$$\frac{\partial^2}{\partial r^2}w_2 + \frac{1}{r}\frac{\partial}{\partial r}w_2 = \frac{\partial}{\partial \eta}w_0 - \frac{\partial^2}{\partial z^2}w_0, \tag{18a}$$

$$\frac{\partial}{\partial r}w_2 = 0, \quad r = r_1; \quad \frac{\partial}{\partial r}w_2 = -\alpha L(w_0), \quad r = 1, \tag{18b}$$

$$w_2 = 0, \quad z = 1; \quad w_2 = 0, \quad \eta = 0, \tag{18c}$$

$$\frac{\partial^2}{\partial r^2}w_3 + \frac{1}{r}\frac{\partial}{\partial r}w_3 = \frac{\partial}{\partial \eta}w_1 - \frac{\partial^2}{\partial z^2}w_1, \tag{19a}$$

$$\frac{\partial}{\partial r}w_3 = 0, \quad r = r_1; \quad \frac{\partial}{\partial r}w_3 = -\alpha \dot{L}(w_0)w_1, \quad r = 1, \tag{19b}$$

$$w_3 = 0, \quad z = 1; \quad w_3 = 0, \quad \eta = 0, \tag{19c}$$

where $\dot{L}$ is the derivative of L with respect to its argument.

The solutions of (17) are $w_0(z, \eta)$ and $w_1(z, \eta)$ for $j = 1$ and $j = 2$ respectively. Both of these functions are unknown at this stage of our analysis. Multiplying (18a) by r, integrating the result from $r = r_1$ to $r = 1$, and applying the boundary conditions (18b) we find that

$$\frac{\partial}{\partial \eta}w_0 = \frac{\partial^2}{\partial z^2}w_0 - \alpha\psi_0^2 L(w_0). \tag{20a}$$

Using this information we find the solution of (18) is

$$w_2 = f_2(z, \eta) - \frac{\alpha}{2}\psi_0^2 L(w_0)\left[\frac{r^2}{2} - r_1^2 \log(r)\right], \tag{20b}$$

where f_2 is unknown at this stage. Similar considerations of (19) give the result

$$\frac{\partial}{\partial \eta}w_1 = \frac{\partial^2}{\partial z^2}w_1 - \alpha\psi_0^2 \dot{L}(w_0)w_1. \tag{21}$$

Summarizing the results to this point our outer expansion is given by

$$u = w_0(z,\eta) + \epsilon w_1(z,\eta) + \epsilon^2 \left\{ f_2(z,\eta) - \frac{\alpha}{2}\psi_0^2 L(w_0)\left[\frac{r^2}{2} - r_1^2 \log(r)\right]\right\} + O(\epsilon^3), \quad (22)$$

where w_0 and w_1 satisfy Equations (20a) and (21), respectively.

3.3. Matching

At this stage of our analysis there are several undetermined quantities which are necessary for the description of the temperature in both the inner and outer regions. In the inner region the functions $a_0(\eta)$ and $a_1(\eta)$ are unknown. These are required to obtain a local approximation to $O(\epsilon)$ there. In the outer region we know that w_0 and w_1 satisfy the one-dimensional heat equations (20a) and (21), respectively. Both of these functions satisfy (17c), *i.e.*, they are zero initially and both satisfy a homogenous Dirichlet condition at $z = 1$. To complete the boundary value problems that each satisfies we need to know their behavior at $z = 0$.

The determination of these unknown quantities is obtained by matching. According to this procedure we expand the inner solution for $\bar{z} >> 1$ and then rewrite the result in terms of the outer variable z. Then we expand the outer solution as $z \to 0$ and compare the two results. The principal of Matched Asymptotics [4] states that these two results must be the same. This equality then determines the unknown quantities.

From (15) we find that the inner expansion for $\bar{z} >> 1$ can be written as

$$\begin{aligned} u = {} & a_0(\eta) - qP_0\mathrm{d}_0\psi_0 z + \frac{\Delta_0}{2}z^2 + \epsilon[a_1(\eta) + qP_0\mathrm{d}_1]\psi_0 + \\ & + \epsilon^2\left[ar + \frac{1}{2}br^2 + a_2(\eta)\psi_0 + \sum_{m=1}^{\infty}\frac{\Delta_m}{\lambda_m}\psi_m\right] + O(\epsilon^3). \end{aligned} \quad (23a)$$

Now the outer result (22) must be expanded as $z \to 0$. Using the Taylor series expansions of both w_0 and w_1 we obtain

$$\begin{aligned} u = {} & w_0(0,\eta) + z\frac{\partial}{\partial z}w_0(0,\eta) + \frac{z^2}{2}\frac{\partial^2}{\partial z^2}w_0(0,\eta) + \cdots + \\ & + \epsilon\left[w_1(0,\eta) + z\frac{\partial}{\partial z}w_1(0,\eta) + \cdots\right] + O(\epsilon^2). \end{aligned} \quad (23b)$$

Comparing these two expansions we find that

$$w_0(0,\eta) = a_0(\eta), \qquad \frac{\partial}{\partial z}w_0(0,\eta) = -q\mathrm{d}_0 P_0\psi_0, \qquad \frac{\partial^2}{\partial z^2}w_0 = \psi_0\Delta_0, \quad (24a,b,c)$$

$$w_1(0,\eta) = [q\mathrm{d}_1 P_0 + a_1(\eta)]\psi_0, \qquad \frac{\partial}{\partial z}w_1(0,\eta) = 0. \quad (24d,e)$$

Now when (24b) is used in conjunction with (17c) and (20a) we obtain a well posed initial boundary value problem for w_0. Similarly, when (24e) is used along with (17c) and (21) we obtain a well posed initial boundary value problem for w_1. In fact the solution of this problem is $w_1 = 0$. This follows because the initial condition and boundary conditions for w_1 are zero and there is no source term in the equation. The matching condition (24d) then yields

$$a_1 = -q\mathrm{d}_1 P_0. \quad (25)$$

Now the initial boundary values problem for w_0 must be numerically solved in general. Once this is done $w_0(0, \eta)$ is determined and $a_0(\eta)$ is obtained from (24a). Inserting this information and (25) into (14) determines the temperature in the inner region to $O(\epsilon)$.

The last thing to check is the condition (24c). By using (20a) evaluated at $z = 0$ and replacing w_0 by u_0 there we find, using the definition of Δ_0 in (13b), that (24c) is an identity. We can push this analysis further and match higher order terms, but we do not do so here.

3.4. The asymptotic model

We briefly restate here the results of our asymptotic analyses for reference and later comparison. Since w_1 is identically zero the temperature in the outer region is given by

$$u = w_0(z, \eta) + O(\epsilon^2), \tag{26}$$

where the $O(\epsilon^2)$ represents the error at this level of approximation. The leading order term satisfies the initial boundary value problem

$$\frac{\partial}{\partial \eta} w_0 = \frac{\partial^2}{\partial z^2} w_0 - \alpha \psi_0^2 L(w_0), \quad 0 < z < 1, \quad \eta > 0, \tag{27a}$$

$$\frac{\partial}{\partial z} w_0 = -q P_0 \mathrm{d}_0 \psi_0, \quad z = 0; \quad w_0 = 0, \quad z = 1, \tag{27b}$$

$$w_0 = 0, \quad \eta = 0, \tag{27c}$$

which must be resolved numerically. We note here that the term driving w_0 is the nonzero Neumann condition (27b) where the right hand side of this boundary condition is the projection of the total microwave power onto the eigenfunction ψ_0. Equation (27) is a one-dimensional heat equation which is clearly easier to solve numerically than the original initial boundary value problem (5). The gain from our asymptotic analysis is not just a reduction in dimension; the original problem is numerically ill-conditioned when $\epsilon << 1$ and (27) is not.

Once w_0 is numerically determined its value at the origin is known. Using this information and (25) we find from (14) that the temperature in the inner region is given by

$$\begin{aligned} u = \; & w_0(0, \eta) - \epsilon q P_0 \left[\int_0^{\bar{z}_c} p S(\chi p) \mathrm{d}p + \int_0^{\bar{z}} (\bar{z} - p) S(\chi p) \mathrm{d}_p \right] \psi_0 + \\ & + \epsilon \sum_{m=1}^{\infty} \frac{q P_m}{\beta_m} \psi_m \left[\cosh \beta_m \bar{z} \int_0^{\bar{z}_c} S(\chi p) \mathrm{e}^{-\beta_m p} \mathrm{d}p - \right. \\ & \left. \int^{\bar{z}_0} \sinh \beta_m (\bar{z} - p) S(\chi p) \mathrm{d}p \right] + \epsilon^2 u_2 + O(\epsilon^3), \end{aligned} \tag{28}$$

where u_2 is given by (13). Thus the determination of the temperature is completely described to $O(\epsilon)$ on the entire physical interval $0 < Z < L$ when (27) is solved numerically.

We now revisit a point that was made in the opening of this section. There we speculated that there might be a boundary layer ($\eta \sim O(\epsilon^2)$) where the inner and outer expansions are not valid. Clearly the outer expansion (26) satisfies the initial condition at $\eta = 0$ by design through (27c). However, the inner expansion only vanishes to $O(\epsilon)$.

We shall briefly describe the method which reconciles this discrepancy and omit the details for brevity. First, we introduce a new short time variable $\bar{t} = \eta/\epsilon^2 \equiv t/\theta_R$ into (4) and seek

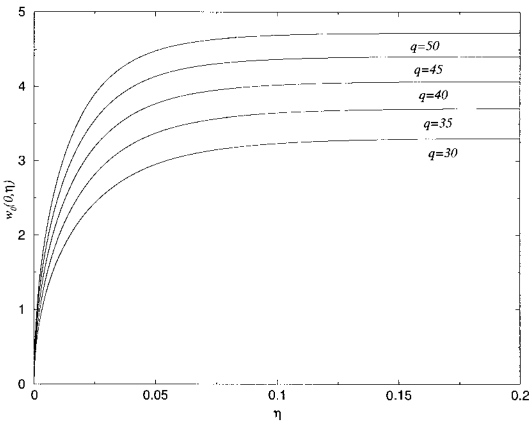

Figure 2. Temperature evolution at the joint. Leading-order asymptotic estimate: $w_0(0, \eta)$.

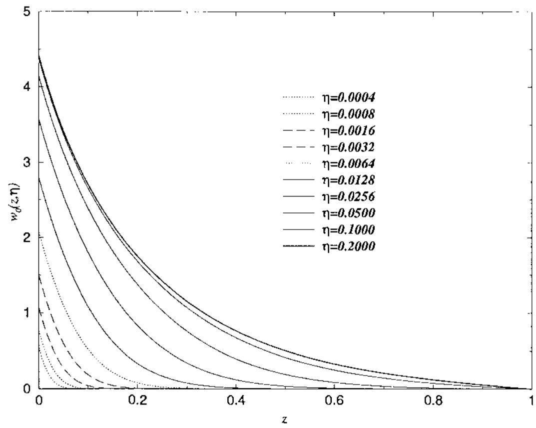

Figure 3. Temperature distribution at various times. Leading-order asymptotic estimate: $w_0(z, \eta)$ with $q = 45$.

another asymptotic expansion of the temperature. This would proceed in exactly the same way as the development of the inner expansion in Section 3.1, except for two differences. First, the expansion would begin with an order ϵ term since this is the size of the source term. More importantly, the sequential boundary value problems are all parabolic and they describe diffusion in the radial and axial directions on the short time scale. Then by expanding this new asymptotic expansion for a fixed $\bar{t}$ and $\bar{z} \to \infty$ we can show that $u \to 0$. This result then matches, as $\bar{t} \to \infty$, into the outer expansion (26) as $\eta \to 0$. Thus, the homogeneous initial condition (27c) is valid. We can also show that this new expansion matches, as $\bar{t} \to \infty$ (28) as $\eta \to 0$. Thus, the initial conditions are transformed by the radial and axial diffusion on the short time scale into the proper function on the long time scale. Finally, we can deduce from this matching that $a_0(\eta) = w_0(0, \eta) \sim 2P_0 \mathrm{d}_0\sqrt{\eta/\pi}$ as $\eta \to 0$, and this is observed in our numerical experiments described below.

4. Numerical example

Using the parameter values stated in Section 2 we find that $\epsilon = 0{\cdot}04$, $\gamma = 1{\cdot}95$, $\chi = 0{\cdot}52$, $\alpha = 1{\cdot}74$, $\beta = 0{\cdot}01$, $r_1 = 0{\cdot}875$, $\psi_0 = 2{\cdot}92$, $\bar{z}_c = 3$, $\theta_C = 3\ hrs$, and $\theta_R = 7$ mins. From the definition of d_0 and d_1, equation (15b), straight forward integration gives $\mathrm{d}_0 = \bar{z}/2 = 1{\cdot}5$, and $\mathrm{d}_1 = (\bar{z}_c^2 - 1/\chi^2)/4 = 1{\cdot}33$. The constant $P_0 = \int_{r_1}^{1} r\psi_0 J_1^2(\gamma r)\mathrm{d}r$ must be solved numerically, its value is $P_0 = 0{\cdot}115$. The only free parameter at this stage is q which from (3b) is seen to be proportional to the microwave power; the flux in (27b) is $-0.5q$.

We have used a finite-difference scheme based on Crank-Nicolson differencing to solve (27) numerically. The nonlinear loss term, $L(w_0)$, is handled by linearizing locally at each time step. We have taken very fine numerical grids to assure that the solution is fully resolved. Figure 2 shows a time history for $w_0(0, \eta)$ for $q = 30, 35, 40, 45, 50$. From (28) this is the lowest order behavior of the inner solution. As expected, the temperature at the origin behaves like $\sqrt{\eta}$ and rises rapidly for small values of η, indeed at an infinite rate initially, due to heat flux imposed at the origin. As convective and radiative losses balance this flux,

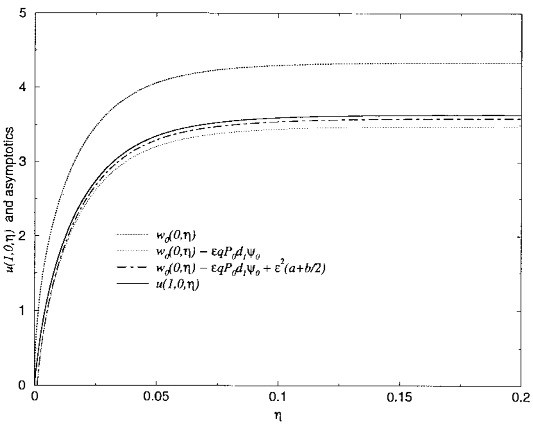

Figure 4. Comparison of $u(1, 0, \eta)$ and asymptotics.

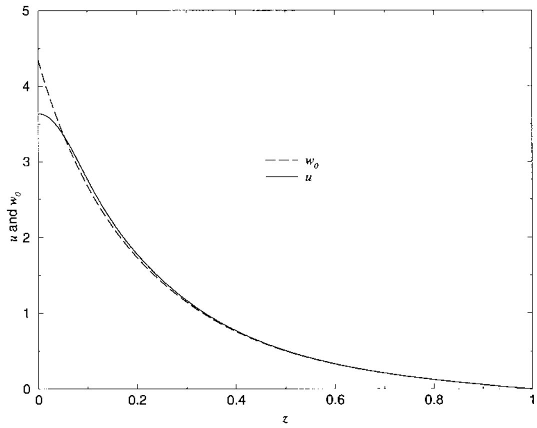

Figure 5. Steady-state surface temperature. Leading-order asymptotics and full simultation.

the temperature at the origin saturates at a steady value which is a monotonically increasing function of q. Figure 3 shows $w_0(z, \eta)$ for various values of η and $q = 45$. Clearly, as η becomes large w_0 goes to a steady state with its maximum temperature at the origin. We note that the steady steate temperature is established more rapidly at $z = 0$ than at points with $z > 0$.

An important question that can be answered at this point is to estimate the power required to obtain a prescribed temperature at the joint, $Z = 0$. For example if the joining temperature is $T_J = 1100\,°\mathrm{C}$, then this corresponds to a dimensionless temperature of $u_J = 3{\cdot}666$ for $T_A = 30\,°\mathrm{C}$. From Figure 2 we see that selecting $q \approx 35$ gives a temperature of about u_J. However, using the higher-order corrections to w_0 given in (28) and (14) can refine this estimate considerably. In applying these corrections, we use the result that the P_m/λ_m's for $m \geq 1$ and $a_2(\eta)$ are negligibly small in our case. Applying the $O(\epsilon)$ correction gives $q \approx 46$; with the $O(\epsilon^2)$ correction, we estimate $q_J = 45$. This result compares favorably with the value of $q_J = 44$ estimated from the direct simulations of (4) discussed in the next section. In dimensional terms the value of $q = 44$ corresponds to about 1040 W.

5. A full numerical simulation

In this section we briefly describe numerical experiments on the full system (4). We treat (4) using an alternating-directions splitting. Diffusion in the r and z directions is treated with Crank-Nicolson differencing. Nonlinear terms are linearized locally. Because of the very large diffusion coefficient in the radial direction extremely small time steps are required. The computational resources, measured in total number of arithmetic operations, required to accurately solve the full system (4) exceed those needed to obtain accurate solutions of the asymptotic model (27) by at least a factor of a thousand. We take $q = 44$ in the following.

In Figure 4 we compare the time histories of the surface temperature at the origin for the full scale simulation and asymptotic analysis. The surface temperature at the origin for the simulation based on (4) is denoted $u(1, 0, \eta)$. The leading order asymptotics $w_0(0, \eta)$ are well above $u(1, 0, \eta)$ for $\eta > 0$. The relative error in the prediction of the steady state temperature is about 20%. The first order correction $w(0,\eta) - \epsilon q P_0 \mathrm{d}_1 \psi_0$ lies below and much closer to $u(1,0,\eta)$. We note that since $w(0,\eta) = 0$ the first order correction gives a negative temperature for very small values of η. Furthermore, we note that the first order correction is insensitive to the nonlinearity in the problem which is measured by β. The relative error in the prediction of the steady state temperature is about 4%. The nonlinearity affects the $O(\epsilon^2)$ correction which gives very good agreement with $u(1,0,\eta)$. The relative error in the prediction of the steady state temperature is about 2%.

In Figure 5 we show the steady state surface temperature obtained from numerical solution of the full system (4) as the solid curve and the steady state temperature distribution from numerical solution of the leading order asymptotic system (27) as the dotted curve. We judge the solutions to have effectively reached steady state when $\eta = 0{\cdot}2$. The two are almost identical for $z \geq 3$ and begin to differ when z is reduced. The difference is at most 2% for $z_c = 1.5 \leq z < 3$, *i.e.*, up to the cavity and the inner region. This excellent agreement between the outer expansion and the numerical simulation there is almost unexpected. Moreover, the outer expansion continues to give an excellent approximation well inside the cavity until the two curves intersect. At this point the inner expansion really must be employed. Because the radiative loss is important here we need the inner expansion to $O(\epsilon^2)$. This is a very complex expression which we will not evaluate at this time for arbitrary $\bar{z}$. The value of this expansion at $\bar{z} = 0$ has been described in the previous section and Figure 4 demonstrates its effectiveness at this point.

6. Conclusion

We have analyzed a nonlinear heat equation which models the microwave assisted joining two large SiC tubes. By exploiting the small fineness ratio of the structure and the disparate time scales θ_R and θ_C we deduced an asymptotic theory for this problem. Specifically, we found that the temperature in the outer region was governed by a one-dimensional nonlinear heat equation. This is a numerically well posed problem and we efficiently solve it using a standard method. This solution is not valid in the inner region which includes the microwave source. We have derived an asymptotic approximation to the temperature in this region. This approximation yielded two unknown functions which were determined from matching and were obtained from the outer solution. We have compared the results of our asymptotic theory to calculations done on the full problem. Since the full problem is numerically ill conditioned, our asymptotic theory yields enormous savings in time and computational effort.

We close this section by making two observations. First, all of our analysis can be generalized to handle the case of temperature dependent thermal and electrical conductivities. If we set $k(u) = K(T)/K(T_A)$ and $f(u) = \sigma(T)/\sigma(T_A)$, then the initial boundary value problem (27) is replaced by

$$\frac{\partial}{\partial \eta} w_0 = \frac{\partial}{\partial z}\left(k(w_0)\frac{\partial}{\partial z} w_0\right) - \alpha \psi_0^2 L(w_0), \quad 0 < z < 1, \quad \eta > 0, \tag{29a}$$

$$k(w_0)\frac{\partial}{\partial z} w_0 = -q f(w_0) P_0 \mathrm{d}_0 \psi_0, \quad z = 0; \quad w_0 = 0, \quad z = 1, \tag{29b}$$

$$w_0 = 0, \quad \eta = 0. \tag{29c}$$

The inner result (28) is modified in a similar fashion. Thus, we again obtain a one-dimensional problem. All of the remarks made above apply to this case. The second observation is that the homogeneous boundary $(\partial/\partial_R)T = 0$ at $R = R_i$ is a very good approximation. In Appendix A we show, under the assumptions that the pipe is a black body and that no air is forced through the inside of the tube, that the asymptotic results presented in this paper are valid to at least $O(\epsilon^2)$.

Acknowledgements

This work was supported by the Air force Office of Scientific Research Under Grant No. AFOSR F49620-94-1-0338, the Department of Energy Under Grant No. DE-FG02-94ER25196, and the National Science Foundation Under Grant No. DMS 9305828. The authors wish to thank Dr. Richard Silberglitt for his encouragement to undertake this work, and for his many helpful and insightful suggestions in its completion.

Appendix A

The dimensionless radiative thermal balance is

$$\frac{\partial}{\partial r}u + \alpha\beta\epsilon^2 \left[(u(r,z,\eta)+1)^4 - \int_{-1}^{1} (u(r,z',\eta)+1)^4 \frac{1}{\epsilon} K\left(\frac{z-z'}{\epsilon}\mathrm{d}\right) z' \right] = 0, \tag{A1a}$$

$$r = r_1$$

where the Kernel is an even function of its argument and satisfies

$$\int_{-1}^{1} \frac{1}{\epsilon} K\left(\frac{z-z'}{\epsilon}\right) \mathrm{d}z' = 1 \tag{A1b}$$

for all ϵ. The kernel is an involved trigonometric integral obtained from a view angle analysis [8] and we do not produce it here. The integral in (A1a) represents the incident heat flux coming from all the interior points of the surface $r = r_1$. If we rewrite (A1a) in terms of the inner variable $\bar{z}$, then we find

$$dis\frac{\partial}{\partial r}u + \alpha\beta\epsilon^2 \left[(u+1)^4 - \int_{-\infty}^{\infty} (u+1)^4 K(\bar{z}-p)\mathrm{d}p \right] = 0, \quad r = r_1. \tag{A2}$$

This will enter the analysis at the $O(\epsilon^2)$ stage by forcing u_2, *i.e.*,

$$\frac{\partial}{\partial r}u_2 + \alpha\beta\epsilon^2 \left[(a_0+1)^4 - \int_{-\infty}^{\infty} (1+a_0)^4 K(\bar{z}-p)\mathrm{d}p \right] = 0, \quad r = r_1. \tag{A3}$$

But a_0 is just a function of η and so by virtue of (A1b) $(\partial/\partial_r)u_2 = 0$ at $r = r_1$. Thus the inner expansion remains the same at least to $O(\epsilon^2)$.

In the outer region (A1a) holds. We observe that $\frac{1}{\epsilon}K((z-z')/\epsilon)$ behaves like a delta function as $\epsilon \to 0$. Thus, the integral picks off $(u+1)^4$ at $z' = z$ and produces a correction term which is proportional to $(\partial^2/\partial z^2)(u+1)^4$ at $z' = z$. The result is

$$\frac{\partial}{\partial r}u + \alpha\beta\epsilon^4 c_1 \frac{\partial}{\partial z}\left[4(u+1)^3 \frac{\partial}{\partial z}u \right] = 0, \quad r = r_1, \tag{A4}$$

where c_1 is an $O(1)$ constant. This implies that the outer expansion will not be affected until the $O(\epsilon^4)$ term. Thus the outer expansion remains the same at least to $O(\epsilon^3)$.

References

1. R. Silberglitt, I. Ahmad, W.M. Black, and J.D. Katz. Recent developments in microwave joining. *Material Res. Soc. Bull*. 18 (1993) 47–50.
2. J.G.P. Binner, P.A. Davis, T.E. Cross, and J.A. Fernie. Microwave joining of engineering ceramics. *Ceram. Trans.* 59 (1995) 335–346.
3. G.A. Danko, R. Silberglitt, and P.S. Day. Joining of Sintered SiC Tubes to SiC/SiC Composites Plates Using Preceramic Polymer with Microwave Hybrid Heating. Indianapolis: 101st Annual Meeting & Exposition of the American Ceramic Society (1999) Paper BS4-016-99.
4. J. Kevorkian and J.D. Cole. *Perturbation Methods and Applied Mathematics*. New York City: Springer-Verlag (1981) 558 pp.
5. H.K. Kuiken and P.J. Roksnoer. Analysis of the temperature in FZ silicon crystals. J. Cryst. Growth 47 (1979) 20–42.
6. G.W. Young and Chait. Steady-state thermal-solutal diffusion in a float zone. *J. Cryst. Growth* 96 (1989) 65–95.
7. S.A. Morman and G.W. Young. An asymptotic approach to the mathematical modeling of Ohno continuous casting of cored rods. *J. Eng. Math.* 38 (2000) 51–76.
8. E.M. Sparrow and R.D. Cess, *Radiation Heat Transfer*. London: Hemisphere Publishing (1978) 366 pp.